Inorganic Chemistry

ARTICLE

pubs.acs.org/IC

Influence of Calcium-Induced Aggregation on the Sensitivity of Aminobis(methylenephosphonate)-Containing Potential MRI Contrast Agents

Jörg Henig,[†,⊥] Ilgar Mamedov,[‡,⊥] Petra Fouskova,[§] Éva Tóth,[§] Nikos K. Logothetis,[‡,∥] Goran Angelovski,[*,‡] and Hermann A. Mayer[*,†]

[†]Institut für Anorganische Chemie, Eberhard Karls Universität Tübingen, Auf der Morgenstelle 18, 72076 Tübingen, Germany

[‡]Abteilung für Physiologie kognitiver Prozesse, Max-Planck-Institut für biologische Kybernetik, Spemannstrasse 38, 72076 Tübingen, Germany

[§]Le Centre de Biophysique Moléculaire, Centre National de la Recherche Scientifique, CNRS, Rue Charles Sadron, 45071 Orléans, France

[∥]Imaging Science and Biomedical Engineering, The University of Manchester, Oxford Road, Manchester M13 9PT, U.K.

Supporting Information

ABSTRACT: A novel class of 1,4,7,10-tetraazacyclododecane-1,4,7-tris(methylenecarboxylic) acid (DO3A)-based lanthanide complexes with relaxometric response to Ca^{2+} was synthesized, and their physicochemical properties were investigated. Four macrocyclic ligands containing an alkyl-aminobis(methylenephosphonate) side chain for Ca^{2+}-chelation have been studied (alkyl is propyl, butyl, pentyl, and hexyl for **L**[1], **L**[2], **L**[3], and **L**[4], respectively). Upon addition of Ca^{2+}, the r_1 relaxivity of their Gd^{3+} complexes decreased up to 61% of the initial value for the best compounds **GdL**[3] and **GdL**[4]. The relaxivity of the complexes was concentration dependent (it decreases with increasing concentration). Diffusion NMR studies on the Y^{3+} analogues evidenced the formation of agglomerates at higher concentrations; the aggregation becomes even more important in the presence of Ca^{2+}. ^{31}P NMR experiments on **EuL**[1] and **EuL**[4] indicated the coordination of a phosphonate to the Ln^{3+} for the ligand with a propyl chain, while phosphonate coordination was not observed for the analogue bearing a hexyl linker. Potentiometric titrations yielded protonation constants of the Gd^{3+} complexes. log K_{H1} values for all complexes lie between 6.12 and 7.11 whereas log K_{H2} values are between 4.61 and 5.87. Luminescence emission spectra recorded on the Eu^{3+} complexes confirmed the coordination of a phosphonate group to the Ln^{3+} center in **EuL**[1]. Luminescence lifetime measurements showed that Ca-induced agglomeration reduces the hydration number which is the main cause for the change in r_1. Variable temperature ^{17}O NMR experiments evidenced high water exchange rates on **GdL**[1], **GdL**[2], and **GdL**[3] comparable to that of the aqua ion.

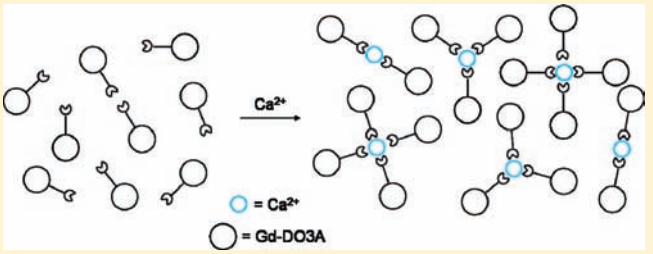

INTRODUCTION

The evolution of magnetic resonance imaging (MRI) into one of the most powerful tools in medical diagnosis is strongly related to the development of paramagnetic contrast agents (CAs). Most commonly, these are based on trivalent gadolinium which has the strongest influence on the relaxation of surrounding water protons.[1,2] Lately, efforts to develop "smart" contrast agents (SCA) have become an important field in MRI research.[3,4] The relaxivity, r_1, of these CAs is responsive to changes in the chemical microenvironment of the Gd^{3+} complex, such as variations in the pH or the concentration of inorganic ions and organic molecules, and so forth (r_1 is the paramagnetic longitudinal proton relaxation rate enhancement referred to one millimolar concentration of Gd^{3+}).

Several pH responsive CAs have been reported,[5−7] some of them already finding in vivo application in the determination of the pH in tumor tissue and the generation of pH maps.[8] In metal ion sensing, most of the efforts have been directed to design gadolinium complexes that are able to report changes in concentrations of the physiologically important Ca^{2+} and Zn^{2+} cations.[9−16] Many CAs developed for the detection of Ca^{2+}, consist of a macrocyclic 1,4,7,10-tetraazacyclododecane-1,4,7-tris(methylenecarboxylic) acid (DO3A) based Gd^{3+} complex which is linked to an additional aminocarboxylate moiety for selective Ca^{2+} coordination. It can be assumed that at least one donor group of this moiety is able to coordinate to the Gd^{3+} center in the absence of Ca^{2+}, whereas in the presence of the divalent metal ion, the donor group dissociates from the Gd^{3+} to complex the sensed metal ion. This reorganization of the complex exposes the gadolinium ion to bulk water, indicated

Received: December 4, 2010
Published: June 14, 2011

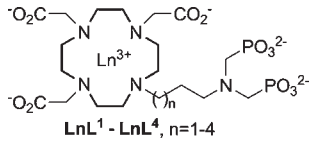

Figure 1. Structures of the investigated DO3A alkylaminobis(methylenephosphonates), $\mathbf{L^1}$, $n = 1$; $\mathbf{L^2}$, $n = 2$; $\mathbf{L^3}$, $n = 3$; $\mathbf{L^4}$, $n = 4$.

by an increase of the number of coordinated water molecules q and resulting in positive change in relaxivity.[15,17]

Very recently we have reported the synthesis and the in vivo characterization of a novel Ca^{2+} sensitive potential MRI CA based on DO3A, which bears an hexylaminobis(methylenephosphonate) group instead of an aminocarboxylate chelator as the Ca^{2+} sensitive binding site ($\mathbf{LnL^4}$ in Figure 1).[18] The aminobis(methylenephosphonate) unit was chosen since the introduction of negatively charged phosphonate groups into common Gd^{3+}-based CAs usually increases their r_1 because of an acceleration of the water exchange rate k_{ex} and their ability to form a second sphere water network around the Gd^{3+} complexes, both factors being important to improve the MR signal, especially in high field magnets.[19−21]Bis(phosphonates) attached to the DO3A core or to superparamagnetic iron oxide (SPIO) particles were already proposed as potential bone targeting CAs.[22,23] Moreover, aminopolyphosphonic acids are well-known chelators for transition metal ions,[24,25] but they also exhibit high complexation efficiency toward biologically important metal ions such as Ca^{2+}, Mg^{2+}, and Zn^{2+}.[26] Initial in vitro physicochemical studies of $\mathbf{GdL^4}$ showed a very untypical Ca^{2+} sensitivity. Namely, the addition of Ca^{2+} ions resulted in a negative change in relaxivity.[18] To investigate this interesting effect more thoroughly, we have prepared three additional analogous compounds which bear a propyl ($\mathbf{L^1}$), butyl ($\mathbf{L^2}$), or pentyl ($\mathbf{L^3}$) linker instead of a hexyl ($\mathbf{L^4}$) one between the aminobis(methylenephosphonates) and DO3A. Here we present an extensive mechanistic investigation of $\mathbf{LnL^1}$−$\mathbf{LnL^4}$.

EXPERIMENTAL SECTION

General Remarks. ^{1}H NMR, ^{13}C{^{1}H} and ^{31}P{^{1}H} NMR spectra were recorded, and the relaxometric measurements were performed on a Bruker DRX400 spectrometer (9.4 T) at room temperature, unless otherwise specified. The ^{1}H PGSE NMR diffusion measurements were performed on a Bruker Avance II+ 500 spectrometer (11.75 T) equipped with a gradient unit and a multinuclear inverse probe with a Z-gradient coil. ^{17}O NMR experiments were performed on a Bruker Avance 500 spectrometer (11.75 T, 67.8 MHz). Luminescence steady-state and lifetime measurements were performed on QuantaMaster 3 PH fluorescence spectrometer from Photon Technology International, Inc., U.S.A. ESI-LRMS were performed on an ion trap SL 1100 system (Agilent, Germany). Column chromatography was performed using silicagel 60 (70−230 mesh ASTM) from Merck, Germany. Experimental details on the synthesis and characterization data of compounds **2d**, **3d**, **4d**, $\mathbf{L^4}$, $\mathbf{GdL^4}$, and $\mathbf{EuL^4}$ have been previously reported.[18]

Synthesis of Ligands and Complexes. *General Procedure for* ***2a*****−****c***. A solution of NaOH (3 equiv) in water (30 mL) was added dropwise to a vigorously stirring biphasic mixture consisting of **1a**−**c** (1.5 equiv) in water (50 mL) and Boc_2O (1 equiv) in 100 mL of dichloromethane. After 3 h the organic phase was separated and washed with a 2 N HCl (50 mL) and a saturated NaCl solution (50 mL). The organic phase was dried over $MgSO_4$ and concentrated in vacuo. *n*-Hexane (20 mL) was added to the oil and the solution was stored at −20 °C for 16 h. The products were separated from the solvent, washed with cold *n*-hexane, and dried in vacuo.

*tert-Butyl 3-Bromopropylcarbamate (**2a**).* Colorless crystals, yield 68%. ^{1}H NMR ($CDCl_3$): δ 5.25 (s, 1H, NH), 3.38 (t, 2H, $^3J_{HH}$ = 6.5 Hz, $BrCH_2$), 3.25 (t, 2H, $^3J_{HH}$ = 6.5 Hz, $NHCH_2$), 1.95 (tt, 2H, $^3J_{HH}$ = 6.5 Hz, $^3J_{HH}$ = 6.5 Hz, CH_2), 1.37 (s, 9H, CH_3). ^{13}C {^{1}H} NMR ($CDCl_3$): δ 155.6 (CO), 79.8 ($C(CH_3)_3$), 38.6, 32.4, 30.4 (CH_2), 27.9 (CH_3). EA Calcd: C 40.35%, H 6.77%, N 5.88%. Found: C 40.29%, H 7.23%, N 5.88%.

*tert-Butyl 5-Bromobutylcarbamate (**2b**).* Yellow crystals, yield 67%. ^{1}H NMR ($CDCl_3$): δ 4.81 (s, 1H, NH), 3.52 (t, 2H, $^3J_{HH}$ = 6.6 Hz, $BrCH_2$), 3.18 (m, 2H, $NHCH_2$), 1.72 (m, 2H, CH_2), 1.32 (s, 9H, CH_3), 1.25−1.40 (m, 2H, CH_2). ^{13}C {^{1}H} NMR ($CDCl_3$): δ 156.3 (CO), 79.4 ($C(CH_3)_3$), 41.1, 32.1, 28.9 (CH_2), 27.7 (CH_3), 24.3 (CH_2). EA Calcd: C 42.87%, H 7.20%, N 5.5%. Found: C 44.18%, H 7.48%, N 5.69%.

*tert-Butyl 5-Bromopentylcarbamate (**2c**).* Yellow oil, yield 65%. ^{1}H NMR ($CDCl_3$): δ 4.92 (s, 1H, NH), 3.52 (t, 2H, $^3J_{HH}$ = 6.7 Hz, $BrCH_2$), 3.25 (m, 2H, $NHCH_2$), 1.94 (tt, 2H, $^3J_{HH}$ = 6.7 Hz, $^3J_{HH}$ = 6.9 Hz, CH_2), 1.32 (s, 9H, CH_3), 1.25−1.40 (m, 4H, CH_2). ^{13}C {^{1}H} NMR ($CDCl_3$): δ 158.3 (CO), 79.8 ($C(CH_3)_3$), 40.5, 33.8, 32.6, 29.4 (CH_2), 28.7 (CH_3), 25.5 (CH_2). EA Calcd: C 45.12%, H 7.57%, N 5.26%. Found: C 45.16%, H 7.20%, N 5.49%.

General Procedure for ***3a*****−****c***. To the solution of 1,4,7-tri(*t*-butoxycarbonylmethyl)cyclen (1 equiv) and K_2CO_3 (1.2 equiv) in acetonitrile (30 mL) was added a solution of **2a**−**c** (1.2 equiv) in acetonitrile (20 mL). After the reaction mixture had been stirred for 16 h at 70 °C, the solution was allowed to cool to room temperature (r. t.), filtered, and concentrated in vacuo to give a yellow to brown oil. The compounds were purified by column chromatography (5% CH_3OH in CH_2Cl_2).

*tri-tert-Butyl 2,2′,2″-(10-(3-(tert-butoxycarbonylamino)propyl)-1,4,7,10-tetraazacyclododecane-1,4,7-triyl)triacetate (**3a**).* Yellow oil, yield 85%. ^{1}H NMR ($CDCl_3$): δ 5.90 (s,1H, NH), 3.60−2.03 (m, 26H, CH_2), 1.29 (m, 2H, CH_2NH), 1.11−1.05 (m, 36H, $C(CH_3)_3$). ^{13}C {^{1}H} NMR ($CDCl_3$): δ 173.6, 172.6 (COOt-Bu), 156.3 (COBoc), 82.7, 82.4, 81.7 ($C(CH_3)_3$), 57.4, 56.4, 55.7, 51.7, 50.2, 49.7, 38.7 (CH_2), 28.4, 28.0, 27.8 ($C(CH_3)_3$), 26.6, 18.3 (CH_2). ESI-MS: for $C_{34}H_{65}N_5O_8$: calcd. $[M+H]^+$ 672.5, found 672.4.

*tri-tert-Butyl 2,2′,2″-(10-(3-(tert-butoxycarbonylamino)butyl)-1,4,7,10-tetraazacyclododecane-1,4,7-triyl)triacetate (**3b**).* Yellow oil, yield 83%. ^{1}H NMR ($CDCl_3$): δ 5.98 (s,1H, NH), 3.50−2.15 (m, 26H, CH_2), 1.33 (m, 4H, CH_2NH), 1.21−1.18 (m, 36H, $C(CH_3)_3$). ^{13}C {^{1}H}w NMR ($CDCl_3$): δ 174.3, 172.9 (COOt-Bu), 157.0 (COBoc), 83.4, 82.9, 81.6 ($C(CH_3)_3$), 59.0, 57.9, 56.7, 52.3, 51.7, 40.1, 49.9, 39.1 (CH_2), 29.1, 28.7, 28.1 ($C(CH_3)_3$), 26.4, 19.3 (CH_2). ESI-MS: for $C_{35}H_{67}N_5O_8$: calcd. $[M+H]^+$ 686.5, found: 686.7.

*tri-tert-Butyl 2,2′,2″-(10-(3-(tert-butoxycarbonylamino)pentyl)-1,4,7,10-tetraazacyclododecane-1,4,7-triyl)triacetate (**3c**).* Yellow oil, yield 85%. ^{1}H NMR ($CDCl_3$): δ 5.22 (s,1H, NH), 3.42−1.64 (m, 26H, CH_2), 1.36−1.32 (m, 36H, $C(CH_3)_3$), 1.14−1.30 (m, 6H CH_2). ^{13}C {^{1}H} NMR ($CDCl_3$): δ 171.6, 170.7 (COt-Bu), 155.7 (COBoc), 81.6, 80.2, 78.3 ($C(CH_3)_3$), 56.1, 55.9, 53.1, 51.9, 51.6, 51.3, 39.9, 33.3, 31.8 (CH_2) 28.0, 27.7, 27.5 ($C(CH_3)_3$), 24.3, 22.8 (CH_2). ESI-MS: for $C_{36}H_{69}N_5O_8$: calcd 700.5 $[M+H]^+$, found: 700.6.

General Procedure for ***4a*****−****c***. Compounds **3a**−**c** (2 mmol) were taken in dichloromethane (20 mL), and trifluoroacetic acid (20 mL) was added carefully. After the mixture had been stirred at r. t. for 24 h, the solvents were removed under reduced pressure. Dichloromethane (40 mL) was added and evaporated off twice to take out the excess of trifluoracetic acid. The same procedure was repeated twice with methanol. The viscous residues were taken up in a minimum amount of methanol and cold ether was added dropwise. The formed precipitates were filtered and resuspended in 3 mL of water. A large excess of acetone (100 mL) was added, and the cloudy solutions were stored at −20 °C for 16 h. Colorless crystalline powders were filtered off, washed with acetone, and dried in vacuo.

dx.doi.org/10.1021/ic1024235 |*Inorg. Chem.* 2011, 50, 6472–6481

*2,2′,2″-(10-(3-Aminopropyl)-1,4,7,10-tetraazacyclododecane-1,4,7-triyl)triacetic Acid (**4a**).* Colorless crystalline powder, yield 64% ^{1}H NMR (D_2O): δ 3.69−2.66 (m, 26H, CH_2), 1.73 (m, 2H, CH_2). ^{13}C {^{1}H} NMR (D_2O): 174.2, 171.2 (COOH), 56.5, 53.8, 51.6, 50.6, 49.7, 48.7, 37.4, 24.9, 24.9 (CH_2). HRMS (EI): for $C_{17}H_{33}N_5O_6$: calcd: 402.3265 $[M\text{-}H]^-$; found: 402.3266.

*2,2′,2″-(10-(3-Aminobutyl)-1,4,7,10-tetraazacyclododecane-1,4,7-triyl)triacetic Acid (**4b**).* Colorless crystalline powder, yield 66%. ^{1}H NMR (D_2O): δ 3.94 (m, 2H, CH_2NH_2), 3.45−2.52 (m, 24H, CH_2), 1.60−1.32 (m, 4H, CH_2). ^{13}C {^{1}H} NMR (D_2O): δ 176.3, 169.8 (COOH), 56.7, 55.3, 54.2, 52.7, 50.4, 49.5, 39.9, 26.9, 23.7, 23.2 (CH_2). ESI-MS: for $C_{18}H_{35}N_5O_6$: calcd: 418.3 $[M+H]^+$; found: 418.0.

*2,2′,2″-(10-(3-Aminopentyl)-1,4,7,10-tetraazacyclododecane-1,4,7-triyl)triacetic Acid (**4c**).* Colorless crystalline powder, yield 62%. ^{1}H NMR (D_2O): δ 3.74 (m, 2H, CH_2NH_2), 3.50−2.64 (m, 24H, CH_2), 1.57−1.21 (m, 6H, CH_2). ^{13}C {^{1}H} NMR (D_2O): δ 174.4, 169.1 (COOH), 55.9, 54.1, 53.2, 51.6, 49.9, 48.5, 48.3, 39.2, 26.3, 22.9, 22.7 (CH_2). HRMS (EI): for $C_{19}H_{37}N_5O_6$: calcd: 430.2671 $[M\text{-}H]^-$; found: 430.2664.

*General Procedure for **L^1**−**L^3**.* Compounds **4a**−**c** (1 equiv) were dissolved in 6 M HCl (10 mL). Phosphoric acid (2 equiv) in water (5 mL) was added to these solutions, and the mixtures were heated to reflux. Paraformaldehyde (4 equiv) was added portionwise within 1 h, and heating under reflux was continued for further 24 h. The reaction mixtures were concentrated under reduced pressure and cold ethanol was added slowly under stirring. The solutions were cooled to −20 °C for 12 h. The solid product was separated by filtration and dried by prolonged standing in vacuo.

*2,2′,2″-(10-(3-(Bis(phosphonomethyl)amino)propyl)-1,4,7,10-tetraazacyclododecane-1,4,7-triyl)triacetic Acid (**L^1**).* Colorless powder, yield 54%. ^{1}H NMR (D_2O): δ 2.20−3.35 (m, 30H), 1.29−1.39 (m, 2H). ^{31}P {^{1}H} NMR (D_2O): δ 10.02. ^{13}C {^{1}H} NMR (D_2O): δ 173.7, 167.7 (COOH), 54.0 (d, $^1J_{PC}$ = 33.6 Hz), 52.9, 52.2, 51.5, 51.4, 50.9, 50.7, 50.1, 48.3, 19.4. HRMS (EI): for $C_{19}H_{39}N_5O_{12}P_2$: calcd: 590.2000 $[M\text{-}H]^-$; found: 590.1985.

*2,2′,2″-(10-(3-(Bis(phosphonomethyl)amino)butyl)-1,4,7,10-tetraazacyclododecane-1,4,7-triyl)triacetic Acid (**L^2**).* Colorless powder, yield 56%. ^{1}H NMR (D_2O): δ 4.01 (m, 2H, $CH_2N(CH_2PO_3H_2)_2$), 2.95−3.70 (m, 28H), 1.35−1.72 (m, 4H). ^{13}C {^{1}H} NMR (D_2O): δ 174.2, 168.0 (COOH), 55.4, 54.4, 53.6, 52.3, 51.7, 50.1, 49.5, 47.3(d, $^1J_{PC}$ = 33.8 Hz), 22.1, 21.9, 21.7. ^{31}P {^{1}H} NMR (D_2O): δ 9.74. HRMS (EI): for $C_{20}H_{41}N_5O_{12}P_2$: calcd: 604.3252 $[M\text{-}H]^-$; found: 604.3249.

*2,2′,2″-(10-(3-(Bis(phosphonomethyl)amino)pentyl)-1,4,7,10-tetraazacyclododecane-1,4,7-triyl)triacetic Acid (**L^3**).* Colorless powder, yield 52%. ^{1}H NMR (D_2O): δ 4.01 (m, 2H, $CH_2N(CH_2PO_3H_2)_2$), 2.85−3.60 (m, 28H), 1.25−1.66 (m, 6H). ^{13}C {^{1}H} NMR (D_2O): δ 174.3, 168.4 (COOH), 55.9, 54.1, 53.8, 52.8, 51.7, 50.5, 49.9, 48.7, 48.1(d, $^1J_{PC}$ = 33.8 Hz), 22.6, 22.5, 22.3. ^{31}P {^{1}H} NMR (D_2O): δ 7.44. HRMS (EI): for $C_{21}H_{43}N_5O_{12}P_2$: calcd: 618.2311 $[M\text{-}H]^-$; found: 618.2310.

General Procedure for the Synthesis of Ln-Complexes. To the water solutions the ligands **L^1**−**L^4** were mixed with the equimolar (referred to the calculated molecular weight of the ligand) amount of the corresponding $LnCl_3$. The mixtures were heated to 60 °C for 24 h. The pH was periodically checked and adjusted to 6.5−7.5 using a 1 M solution of NaOH. After 24 h the reaction mixture was cooled to room temperature. An anion exchange resin (Chelex 100) was added to the stirring solution, the suspensions were filtered after 1 h, and the solvent evaporated. The absence of the noncoordinated metal ions in the systems was confirmed by the xylenol test. The remaining residue was dissolved in a defined amount of water, and for the gadolinium and europium complexes the metal concentration was determined by measuring the bulk magnetic susceptibility shifts (BMS).[27] From these results the concentrations of the analogously prepared yttrium complex solutions were estimated.

Relaxometric Ca^{2+} Titrations. The titrations were performed at 9.4 T, 25 °C, and pH 7.3−7.4 (maintained by HEPES buffer). A solution of $CaCl_2$ of known concentration was added stepwise to the complex solution, and the longitudinal proton relaxation time T_1 was measured after each addition of the analyte. The relaxivity r_1 was calculated from eq 1, using the actual Gd^{3+} concentration at each point of the titration.

$$\frac{1}{T_{1,\mathrm{obs}}} = \frac{1}{T_{1,\mathrm{d}}} + r_1 \times [\mathrm{Gd}] \qquad (1)$$

where $T_{1,obs}$ is the observed longitudinal relaxation time, $T_{1,d}$ is the diamagnetic contribution in the absence of the paramagnetic substance, and [Gd] is the concentration of Gd^{3+}.

NMR Diffusion Experiments. Appropriate amounts of **YL^1** and **YL^4** were dissolved in D_2O and in a solution of 3 equiv of $CaCl_2$, respectively. The samples were diluted stepwise while keeping the pD at 7.2−7.4. The measurements were performed by using the standard stimulated echo pulse sequence. The temperature was 298 K, and the sample was not spun. The shape of the gradient pulses was rectangular, their duration (δ) was between 1.4 and 1.8 ms, depending on the sample, and their strength (G) was varied during the experiments. The delay between the midpoints of the gradients (Δ) was set to 200 ms. The spectra were recorded using 32−1k scans, 32K points, a relaxation delay of 1.4−3.8 s, a spectral width of 7500 Hz, and were processed with a line broadening of 2. The intensity of the ^{1}H resonances of the alkyl groups of the side chain was determined in all spectra. The plots of $\ln(I/I_0)$ versus G^2 were fitted using a linear regression algorithm to obtain the D values according to eq 2, where I = intensity of the observed spin-echo, I_0 = intensity of the spin-echo without gradients, γ = magnetogyric ratio, δ = length of the gradient pulse, D = diffusion coefficient, Δ = delay between the midpoints of the gradients, and G = gradient strength.

$$\ln\frac{I}{I_0} = -(\gamma\delta)^2 D\left(\Delta - \frac{\delta}{3}\right)G^2 \qquad (2)$$

Potentiometric titrations were carried out in a cell thermostatted at 25 °C, at ionic strength I(KCl) = 0.1 mol·dm^{-3} and in the presence of extra HCl in the $-\log[H^+]$ range 3.8−11, using a combined glass electrode (LL Biotrode, Metrohm) connected to a Metrohm 827 pH/ion-meter, equipped with a Metrohm Dosimat 765 automatic buret. The initial volume was 3 mL, the concentration of the Gd^{3+} complex was 0.001 mol·dm^{-3}. An inert atmosphere was ensured by constant passage of N_2 through the solution. The H^+ concentration was obtained from the measured pH values according to the method proposed by Irving et al.[28] The protonation and stability constants were calculated with the program PSEQUAD.[29] The errors given correspond to one standard deviation. The protonation constants β_n are defined by β_n = $[H_nL]/([H]^n \times [L])$, therefore $\log K_{H1} = \log \beta_1$, $\log K_{H2} = \log \beta_2 - \log \beta_1$. The stability constant is defined by $\beta_{pqr} = [M_pH_qL_r]/([M]^p \times [H]^q \times [L]^r)$.

Luminescence Lifetime Experiments. The decay experiments were performed in H_2O and D_2O (25 °C, pH 7.3, HEPES) on **EuL^1**−**EuL^3** at concentrations ranging from 5 to 50 mM. The Eu^{3+} ion was directly excited at 395 nm and emission intensity at 615 nm was recorded with 10 μs resolution. Excitation and emission slits were set to 15 and 5 nm bandpass, respectively. Data sets are the average of 25 scans, and each reported value is the mean of three independent measurements. Obtained curves are fitted to the first order exponential decay with r^2 = 0.99. q values are calculated using eq 3.

$$q = 1.2 \times (\tau^{-1}_{H_2O} - \tau^{-1}_{D_2O} - 0.25) \qquad (3)$$

^{17}O NMR Spectroscopy. The longitudinal $(1/T_1)$ and transverse $(1/T_2)$ ^{17}O NMR relaxation rates were measured for compounds **GdL$^{1-4}$** in the temperature range of 275−350 K. The concentration

dx.doi.org/10.1021/ic1024235 |*Inorg. Chem.* 2011, 50, 6472–6481

Scheme 1[a]

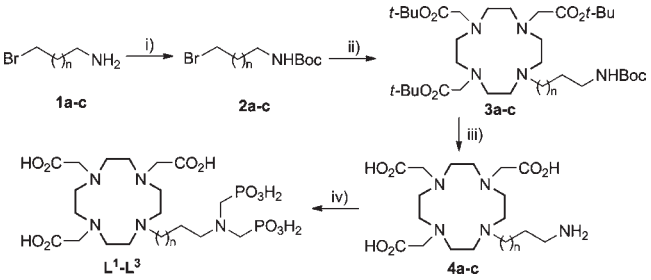

[a] (i) Boc_2O, H_2O/CH_2Cl_2, 62-65%; (ii) tris-*t*-Bu-DO3A, K_2CO_3, CH_3CN, 80 °C, 83-85%; (iii) TFA, CH_2Cl_2, 62-66%; (iv) H_3PO_3, formaldehyde, H_2O, 100 °C, 52-56%.

of the samples was 50 mM and the pH of the solutions was adjusted to 6 using KOH/HCl. The exact Gd^{3+} concentration was determined using the BMS method. The samples were sealed in glass spheres to eliminate the influence of the bulk magnetic susceptibility.[30,31] The exact temperature was calculated according to previous calibration with ethylene glycol and methanol.[32] The $1/T_1$-data were obtained by the inversion recovery method, while the $1/T_2$-data were measured by the Carr−Purcell−Meiboom−Gill spin-echo technique. Acidified water ($HClO_4$, pH 3.3) was used as external reference. The least-squares fit of the ^{17}O NMR data was performed by using Micromath Scientist version 2.0 (Salt Lake City, UT, U.S.A.). The reported errors correspond to one standard deviation obtained by the statistical analysis.

RESULTS AND DISCUSSION

Synthesis of Ligands and Complexes. The ligands $\mathbf{L^1}$−$\mathbf{L^3}$ were synthesized according to Scheme 1, and $\mathbf{L^4}$ according to the protocol described previously.[18] Aminoalkyl alcohols were brominated with HBr/acetic acid solutions using a modified procedure previously published to give **1a**−**c**.[33] Amino groups of **1a**−**c** were protected using Boc_2O at basic conditions to yield **2a**−**c**. The *tert*-butyl ester of DO3A was alkylated with the corresponding Boc-protected bromoalkylamines to give **3a**−**c**. All protective groups on acids and the amine were removed in a one step reaction using trifluoroacetic acid in dichloromethane. Compounds **4a**−**c** were obtained after recrystallization from diethyl ether followed by recrystallization with acetone. The methylenephosphonates were attached to the amines on the side chains by a Mannich reaction using phosphorous acid and formaldehyde at 100 °C.[34] After recrystallization from water/ethanol or water/isopropanol, the final ligands $\mathbf{L^1}$−$\mathbf{L^3}$ were obtained as colorless powders. The excess of phosphoric acid was removed by several recrystallizations, and the process was followed with ^{31}P NMR spectroscopy. The obtained ligands were characterized by ^1H, ^{13}C, ^{31}P NMR spectroscopy and HRMS spectrometry. All final compounds contained a characteristic doublet in the $^{13}C\{^1H\}$ NMR spectrum which is due to the interaction of the carbon atom next to the phosphonate group with the corresponding phosphorus nucleus.

The metal complexes of $\mathbf{L^1}$−$\mathbf{L^3}$ with Gd^{3+}, Eu^{3+}, or Y^{3+} and $\mathbf{YL^4}$ were formed by mixing the corresponding stock solutions of the metal ions with the respective ligands in a 1:1 ratio. The solutions were heated to 60 °C for 24 h while the pH was maintained at ∼7. The complexes were finally treated with Chelex 100, filtered and lyophilized. The xylenol orange test was performed to ensure that there are no free metal ions in the solution. The formation of the complexes was confirmed by ESI-MS spectrometry in negative and positive mode. The appropriate molecular ion peaks with the characteristic isotope pattern of the complexes were present in the analyzed spectra.

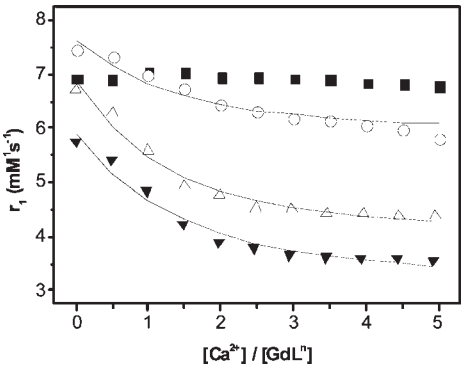

Figure 2. Relaxometric Ca^{2+} titration curves of $\mathbf{GdL^1}$ (■), $\mathbf{GdL^2}$ (○), $\mathbf{GdL^3}$ (Δ) and $\mathbf{GdL^4}$ (▼)[18] at [**GdL**] = 2.5 mM, 9.4 T, 25 °C, pH 7.3 (HEPES buffer). The lines correspond to the fitted curves.

Relaxivity Experiments. Initially, the paramagnetic response of the complexes $\mathbf{GdL^1}$−$\mathbf{GdL^3}$ to physiologically relevant metal ions was studied by means of relaxometric titrations at complex concentrations of 2.5 mM (9.4 T, 25 °C). The experimental data were compared with the experimental results for the complex $\mathbf{GdL^4}$.[18] Already in the absence of any divalent metal ion, the relaxivities of the complexes vary as a function of the length of the pendant arm. r_1 values of 6.92, 7.43, 6.70, and 5.76 mM^{-1} s^{-1} were determined for $\mathbf{GdL^1}$, $\mathbf{GdL^2}$, $\mathbf{GdL^3}$, and $\mathbf{GdL^4}$, respectively.

Significant differences were observed in the r_1 response of $\mathbf{GdL^1}$−$\mathbf{GdL^4}$ to Ca^{2+} (Figure 2). Namely, the sensitivity of the complexes toward Ca^{2+} increases with the extension of the aliphatic side chain. No significant changes in r_1 of $\mathbf{GdL^1}$ were found over the whole span of Ca^{2+} concentration. In the case of $\mathbf{GdL^2}$, a moderate decrease of r_1 was observed on addition of Ca^{2+}, whereas r_1 of the $\mathbf{GdL^3}$ and $\mathbf{GdL^4}$ solutions showed a strong dependence on the calcium concentration resulting in a decrease to 66% and 61% of the initial r_1 values, respectively. The fitting of the curves gave the apparent association constants of log $K_A = 1.6 \pm 0.3$, log $K_A = 1.5 \pm 0.2$, and log $K_A = 2.0 \pm 0.2$ for $\mathbf{GdL^2}$, $\mathbf{GdL^3}$, and $\mathbf{GdL^4}$, respectively. Note that these apparent equilibrium constants are only valid for the specific $\mathbf{GdL^n}$ concentration. The constants give information about the calcium concentration range where the $\mathbf{GdL^n}$ complexes (in millimolar concentration) have a relaxometric response. Upon addition of equimolar amounts of EDTA after the titration of $\mathbf{GdL^3}$ and $\mathbf{GdL^4}$ with Ca^{2+}, the relaxivity of both complexes returned to the initial values obtained in Ca^{2+}-free solutions, indicating that r_1 changes are reversible and exclusively induced by Ca^{2+}.

Relaxometric titrations of $\mathbf{GdL^3}$ and $\mathbf{GdL^4}$ with Mg^{2+} did not show any change in r_1. These complexes, however, exhibit a certain sensitivity to Zn^{2+} ions, though the Zn^{2+} concentrations needed to reach saturation of r_1 are much higher than those of Ca^{2+} (>8 equiv of Zn^{2+} vs <3 equiv of Ca^{2+}) and the addition of EDTA did not lead to a recovery of the initial r_1.

Concentration Dependent Relaxivities. The relaxivity decrease observed for $\mathbf{GdL^2}$−$\mathbf{GdL^4}$ upon addition of Ca^{2+} is unusual and not explainable with the mechanism assumed for the previously reported Ca^{2+} responsive SCAs. Phosphonates, diphosphonates, and aminobis(methylenephosphonates) are able to form aggregates in solution, either hydrogen bonded

dx.doi.org/10.1021/ic1024235 |*Inorg. Chem.* 2011, 50, 6472–6481

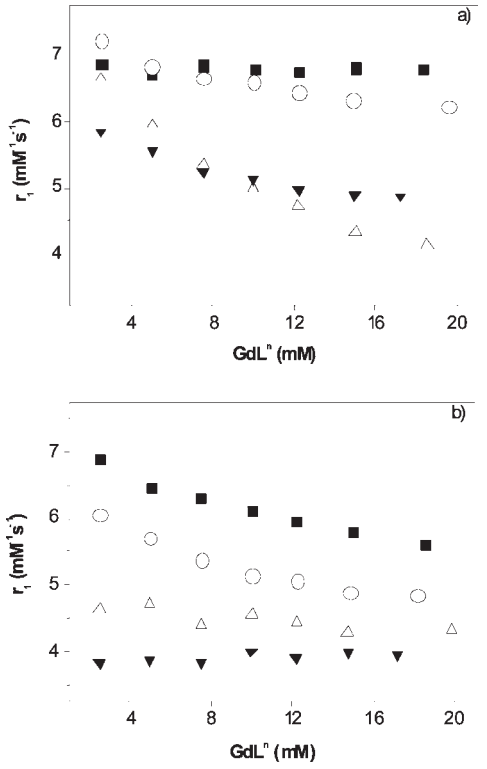

Figure 3. Concentration-dependence of r_1 for **GdL^1** (■), **GdL^2** (○), **GdL^3** (Δ), and **GdL^4** (▼)[18] in (a) the absence of Ca^{2+} and (b) the presence of 3 equiv of Ca^{2+} at 9.4 T, 25 °C, pH 7.3 (HEPES buffer).

(units with two or more molecules) or metal-assisted,[25,35] which might have an influence on the relaxivity. As the ratio between aggregated and non aggregated complexes should be concentration dependent, the relaxivity was studied as a function of the **GdL^1**−**GdL^4** concentration, in the presence and absence of Ca^{2+}. In Ca^{2+}-free solutions only **GdL^1** showed concentration independent relaxivities, while for **GdL^2**−**GdL^4**, the r_1 values were found to be concentration dependent (Figure 3a). The r_1 of **GdL^2**, **GdL^3**, and **GdL^4** dropped by 14, 38, and 17%, respectively, when the complex concentration was increased from 2.5 to 20 mM. However, when the same experiment was performed in the presence of 3 equiv of Ca^{2+}, the change in r_1 for **GdL^3** and **GdL^4** was low, while r_1 decreased by 19 and 20% for **GdL^1** and **GdL^2**, respectively (Figure 3b).

PGSE Measurements. Pulsed gradient spin echo (PGSE) ^{1}H NMR diffusion measurements were performed to confirm that the changes in relaxivity are the result of an aggregation/disaggregation process. Over the past years, this method has shown to be a powerful tool in the elucidation of aggregation processes[36−40] as well as for the determination of global rotational correlation times τ_{Rg}.[41,42] Since complexes of the paramagnetic Gd^{3+} are not suitable for such measurements, the corresponding diamagnetic Y^{3+} complexes were applied. The diffusion coefficients D of the complexes **YL^1** and **YL^4** were determined in the same range of concentration as were used for the concentration dependent relaxivity measurements, both in the absence and presence of Ca^{2+} ions at 25 °C (Figure 4). For comparison, D of the Y^{3+} complex of compound **4d** was also ascertained.

As mentioned above, aggregation is a concentration dependent process. Hence, for an infinitely diluted sample the determined diffusion coefficient D is that of the monomer, whereas in

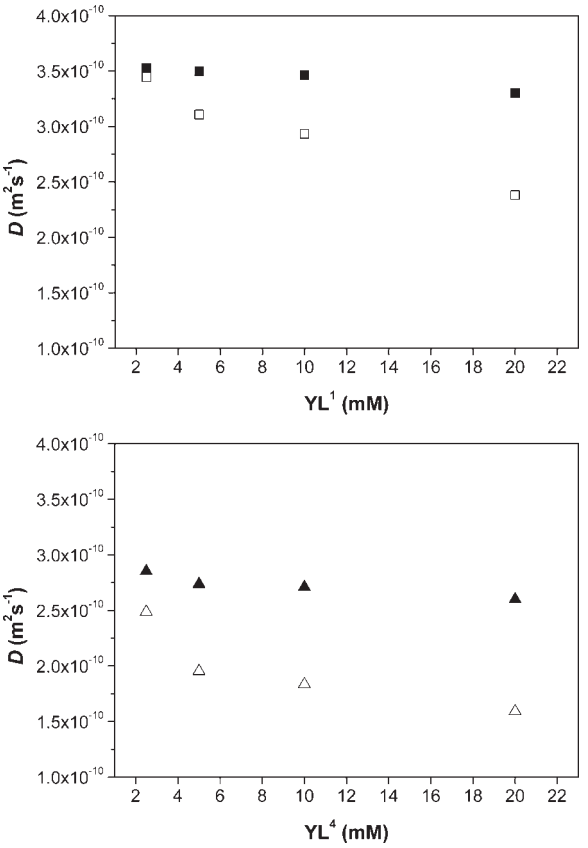

Figure 4. Concentration-dependence of the diffusion coefficient for **YL^1** (top), and **YL^4** (bottom) in the absence of Ca^{2+} (full symbols) and the presence of 3 equiv of Ca^{2+} (empty symbols) at 11.75 T, 25 °C, pH 7.3 (HEPES buffer).

highly concentrated samples D corresponds to that of the aggregate. In samples with concentrations between those two extremes only an average D is determined corresponding to mixtures of aggregated, partly aggregated, and monomeric species. For the quantification of aggregation processes usually the viscosity independent hydrodynamic volume V_H is used.[38] V_H can be calculated from the hydrodynamic radius r_H which is, for spherical molecules, related to the diffusion coefficient D via the Stokes−Einstein equation (eq 4), where k_B is the Boltzmann constant, T is the absolute temperature, η is the viscosity, and r_H is the hydrodynamic radius. Additionally, the global rotational correlation time τ_{Rg} can be calculated from r_H using eq 5.

$$D = \frac{k_B T}{6\pi\eta r_H} \quad (4)$$

$$\tau_{Rg} = \frac{4\pi\eta r_H^3}{3k_B T} \quad (5)$$

Assuming dilute solutions where $\eta_{solution} = \eta_{solvent}$, values for r_H, τ_{Rg}, and V_H were calculated from the obtained diffusion constants (Table 1).

Here, these values should only be regarded as approximations and serve mainly for visualization purposes, as not all complexes and possible aggregates can be considered as spherical. However, it is unambiguous that in the absence of Ca^{2+} the diffusion constants of **YL^1** are significantly higher than those of **YL^4**. The calculated hydrodynamic volume V_H of **YL^4** is about twice the

dx.doi.org/10.1021/ic1024235 |*Inorg. Chem.* 2011, 50, 6472–6481

Table 1. Diffusion Coefficients *D* of Y-4d, YL^1, and YL^4 at Various Concentrations in the Absence of Ca^{2+} and the Presence of 3 equiv of Ca^{2+} at 9.4 T, 25 °C, pH 7.3 (HEPES)

		concentration			
	complex	2.5 mM	5 mM	10 mM	20 mM
D [m^2s^1]	**Y-4d**	3.85×10^{-10}	3.85×10^{-10}	3.85×10^{-10}	3.85×10^{-10}
	$\mathbf{YL^1}$	3.53×10^{-10}	3.50×10^{-10}	3.46×10^{-10}	3.30×10^{-10}
	$\mathbf{YL^1}$ + 3 equiv of Ca^{2+}	3.45×10^{-10}	3.11×10^{-10}	2.93×10^{-10}	2.38×10^{-10}
	$\mathbf{YL^4}$	2.85×10^{-10}	2.74×10^{-10}	2.71×10^{-10}	2.60×10^{-10}
	$\mathbf{YL^4}$ + 3 equiv of Ca^{2+}	2.49×10^{-10}	1.95×10^{-10}	1.84×10^{-10}	1.59×10^{-10}
r_H [Å][a]	**Y-4d**	5.01	5.01	5.01	5.01
	$\mathbf{YL^1}$	5.47	5.52	5.57	5.84
	$\mathbf{YL^1}$ + 3 equiv of Ca^{2+}	5.60	6.21	6.58	8.10
	$\mathbf{YL^4}$	6.76	7.05	7.12	7.42
	$\mathbf{YL^4}$ + 3 equiv of Ca^{2+}	7.75	9.87	10.51	12.12
V_H [$Å^3$][b]	**Y-4d**	528	528	528	528
	$\mathbf{YL^1}$	684	702	725	835
	$\mathbf{YL^1}$ + 3 equiv of Ca^{2+}	736	1003	1192	2228
	$\mathbf{YL^4}$	1295	1465	1511	1711
	$\mathbf{YL^4}$ + 3 equiv of Ca^{2+}	1953	4031	4867	7454
τ_{Rg} [ps][a]	**Y-4d**	145	145	145	145
	$\mathbf{YL^1}$	188	193	199	230
	$\mathbf{YL^1}$ + 3 equiv of Ca^{2+}	202	276	328	613
	$\mathbf{YL^4}$	356	403	416	471
	$\mathbf{YL^4}$ + 3 equiv of Ca^{2+}	537	1109	1339	2050

[a] Calculated from eq 1 using $\eta = 1.13 \times 10^{-3}$ Pa s for D_2O. [b] Calculated from r_H with $V_H = 4/3\pi r_H^3$.

volume of $\mathbf{YL^1}$, whereas V_H of $\mathbf{YL^1}$ is only slightly larger than that of the monomeric **Y-4d**. This confirms the presence of aggregates for $\mathbf{LnL^4}$ already in the absence of Ca^{2+}. *D* of $\mathbf{YL^4}$ and all related parameters are therefore only average values over all forms of $\mathbf{YL^4}$ in solution. The aggregation process is also shown by the increase in V_H of $\mathbf{YL^4}$ with higher complex concentrations, at which the equilibrium between aggregated and monomeric species is shifted toward the aggregated complexes. As, on the other hand, the relaxivity of $\mathbf{GdL^4}$ is decreasing with increasing complex concentration, r_1 of these aggregates must be smaller than r_1 of the monomeric complex.

The tendency of $\mathbf{LnL^1}$ to form aggregates is much lower resulting in a significantly lower hydrodynamic volume. However, in contrast to the relaxivity measurements, V_H of $\mathbf{YL^1}$ shows a small dependence on complex concentration especially at higher concentrations. Therefore, it might be possible that a certain amount of weak aggregates is formed at higher concentrations of $\mathbf{LnL^1}$, but they do not seem to influence the relaxivity. The addition of 3 equiv of Ca^{2+} to $\mathbf{LnL^1}$ then clearly induces aggregation. V_H of $\mathbf{YL^1}$ at c = 20 mM in the presence of Ca^{2+} (3 equiv) is about three-times higher than V_H of $\mathbf{YL^1}$ in the absence of Ca^{2+}. However, at c = 2.5 mM the hydrodynamic volume of $\mathbf{YL^1}$ with Ca^{2+} is only slightly larger than without Ca^{2+}. This implies that Ca^{2+} does not significantly increase the amount of aggregates at this concentration, which can be an explanation for the independence of r_1 on the Ca^{2+} concentration in the initial r_1 measurements at lower Gd^{3+} complex concentrations (2.5 mM). The ratio of the aggregated to nonaggregated complexes increases at higher concentrations of Ca^{2+} which in turn results in the observed decrease in relaxivity.

The addition of Ca^{2+} ions to solutions containing $\mathbf{YL^4}$ increases the hydrodynamic volume even more than in the case of $\mathbf{YL^1}$. The V_H of $\mathbf{YL^4}$ at c = 2.5 mM in the presence of Ca^{2+} is 1.5 times bigger than without Ca^{2+}. As for $\mathbf{LnL^1}$, the increased formation of aggregates seems to be responsible for the decrease in relaxivity of $\mathbf{LnL^4}$. With increasing complex concentration the average size of the species in solution seems to further increase. However, no influence on r_1 was observed for $\mathbf{GdL^4}$ in the concentration dependent experiments (Figure 3b).

The results indicate that Ca^{2+} generally amplifies the formation of aggregates of these systems. Up to a certain point, the formation of bigger aggregates results in the observed decrease in relaxivity. Even though the formation of aggregates leads to a slower rotation (see τ_{Rg} in Table 1), its relaxivity enhancing effect should not be too strong at this high field (9.4 T),[43] and in those cases where r_1 decreases an opposite effect must be also operative.

^{31}P NMR Spectroscopy. To understand whether the different tendencies to form aggregates are related to differences in the interaction of the phosphonate-containing side arms with the paramagnetic center, $^{31}P\{^1H\}$ NMR experiments on $\mathbf{EuL^1}$ and $\mathbf{EuL^4}$ solutions (50 mM in D_2O) were performed (see Supporting Information). The europium complexes are usually used to obtain information on the coordination behavior of the gadolinium analogues by NMR spectroscopy because of their favorable ratio between paramagnetic induced shift and line broadening. The $^{31}P\{^1H\}$ NMR spectrum of $\mathbf{EuL^4}$ (pD 7.4, 298 K) shows only one signal at 6.8 ppm. As this is nearly at the same position as the ^{31}P signal of the free ligand (6.6 ppm at pD 7.4), both phosphonate groups of $\mathbf{LnL^4}$ are most likely not coordinated to the lanthanide ion. The addition of Ca^{2+} results in a broadening of the signal but not in a change of the chemical shift. As for $\mathbf{LnL^4}$ none of the phosphonate groups interact with the lanthanide ion, both groups can interact with calcium. This allows the formation of aggregates involving one or even more Ca^{2+} ions.

dx.doi.org/10.1021/ic1024235 |*Inorg. Chem.* 2011, 50, 6472–6481

Table 2. Protonation Constants of GdL^1-GdL^4 Complexes

	GdL^1	GdL^2	GdL^3	GdL^4
$\log K_{H1}$	6.12 ± 0.01	6.60 ± 0.01	6.96 ± 0.01	7.11 ± 0.03
$\log K_{H2}$	4.61 ± 0.01	5.17 ± 0.01	4.80 ± 0.01	5.87 ± 0.03

In the case of **EuL^1**, the $^{31}P\{^1H\}$ NMR spectrum measured at 298 K displays three resonances, two major signals at 3.1 and 102.3 as well as a minor one at 109.6 ppm. The lanthanide induced shift decreases rapidly with the number of bonds and the distance between the Ln^{3+} ion and the nucleus under study, respectively. Thus the presence of the two strongly upfield shifted resonances suggests an interaction of phosphonate groups with the paramagnetic Eu^{3+} while the signal at 3.1 ppm indicates the existence of phosphonate species which are not coordinated to the paramagnetic center. This allows the conclusion that one of the two phosphonate groups of the aminobis(methylenephosphonate) arm is interacting with the Eu^{3+} center in **EuL^1**.

The two upfield shifted signals merge into one broadened peak when the temperature is increased to 320 K, which can be explained by the existence of two different coordination isomers at lower temperatures.[22,44] Moreover, when the temperature is further increased, the signals of the free and the coordinated phosphonates keep broadening and move closer to each other demonstrating an equilibrium between coordinated and non coordinated phosphonates. Unfortunately, from these data it cannot be concluded whether there is only one species in solution having one coordinated and one uncoordinated phosphonate group which interchange or if there is also a certain amount of complexes whose phosphonates are both non coordinated. Since the diffusion measurements indicated a weak tendency to form aggregates at higher complex concentrations, as are required for the $^{31}P\{^1H\}$ NMR measurements, an intermolecular interaction cannot be excluded, as well. However, after the addition of 3 equiv of Ca^{2+}, the $^{31}P\{^1H\}$ NMR spectrum of **EuL^1** shows a signal at 3.9 ppm and still two upfield shifted resonances, now at -104.3 and -131.6 ppm, respectively. Since the addition of Ca^{2+} affects the chemical shift of the signals corresponding to coordinated phosphonate groups, the aminobis(methylenephosphonate) group of **LnL^1** must be able to interact with Ca^{2+} while one phosphonate group is still coordinated to the Ln^{3+}.

Potentiometric Titrations. Generally, phosphonic acids first protonate at slightly acidic pH ($\log K_{H1} = 5-7$) while the second protonation occurs at considerably lower pH ($\log K_{H2} \leq 2$). The studied Gd^{3+} complexes possess four protonation sites on the two phosphonate groups. Because of the low stability of Gd^{3+} complexes at very acidic pH, the titrations could not be carried out at pH < 4; therefore, the two more acidic protonation constants could not be determined (Table 2). Both protonation constants determined for each system lie in the pH range 4.6–7.1. It can therefore be expected that one protonation step occurs on each of the phosphonates. A general trend is an increase of the protonation constant with the increasing length of the linker between the macrocycle and the bis(phosphonate) group. This can be explained by a change of the electron density on the tertiary amine in the proximity of the phosphonates, which influences their basicity. Note that the increase of the protonation constant is more pronounced from **GdL^1** to **GdL^2** than for the further steps. This can be related to the fact that the metal coordination of the phosphonate in **GdL^1** also contributes to the increased acidity of the phosphonate (see above). Corresponding titration curves are depicted in the Supporting Information. According to these protonation constants, the complexes of **GdL^{1-4}** are partially protonated at physiological pH on one of the phosphonate groups, with the molar fraction of the protonated species varying from a few percent for **GdL^1** to ~30% for **GdL^4**. It should be noted that the nitrogen of the aminobis(phosphonate) group likely remains protonated until a pH above 12, as previously reported for other aminobis(methylenephosphonic acids).[26]

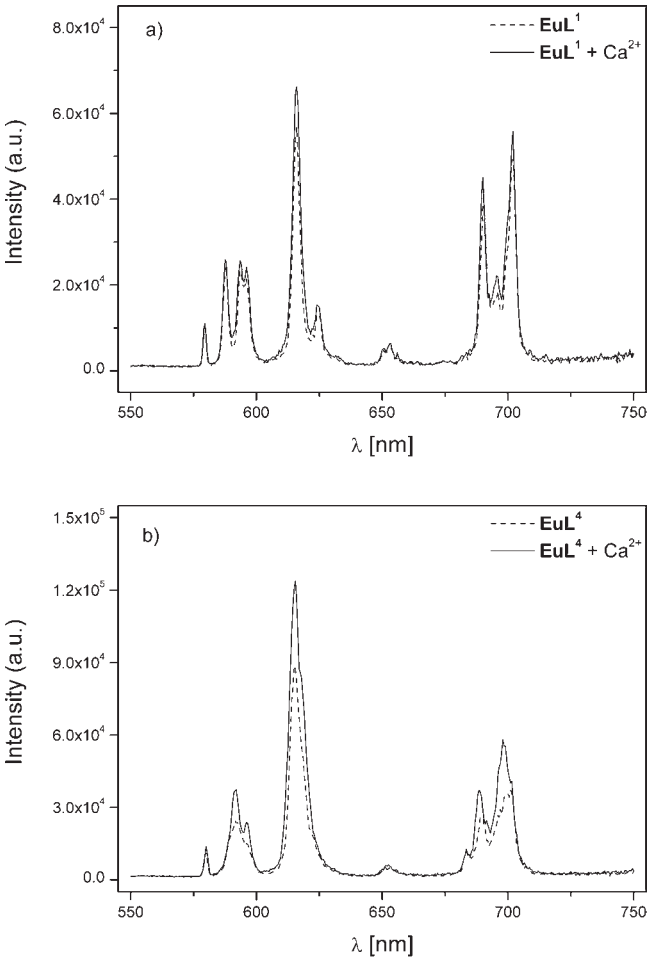

Figure 5. Luminescence emission spectra of **EuL^1** (a) and **EuL^4** (b) in the presence and absence of 3 equiv of Ca^{2+} (5 mM, λ_{ex} = 395 nm, 25 °C, pH 7.3, HEPES).

Luminescence Spectroscopy. Luminescence emission spectra of **EuL^1-EuL^4** in aqueous media give further details about their coordination environment. An advantage of this technique is the possibility to measure at much lower complex concentrations than that required for $^{31}P\{^1H\}$ NMR spectroscopy. This allows observing concentration dependent changes. For **EuL^1**, the coordination of a phosphonate group in the absence and presence of Ca^{2+} could be confirmed for all measured complex concentrations (5 mM–50 mM). The appearance of a distinctive band at 625 nm and the form and splitting of the $\Delta J = 1$ manifold suggest coordination of the europium with the phosphonate group[45,46] (Figure 5a). Since the coordination can be observed also at low complex concentrations where the diffusion measurements indicated no significant aggregation, it is much more likely that the coordination to the lanthanide(III) ion is an

dx.doi.org/10.1021/ic1024235 |Inorg. Chem. 2011, 50, 6472–6481

Table 3. Luminescence Emission Lifetimes and Estimated q Values of EuL^1−EuL^4 (4−5 mM) in the Absence and Presence of Ca^{2+} (3 equiv)

complex	q	complex + Ca^{2+}	q
EuL^1	1.7	EuL^1 + 3 equiv of Ca^{2+}	1.2
EuL^2	1.0	EuL^2 + 3 equiv of Ca^{2+}	0.7
EuL^3	1.4	EuL^3 + 3 equiv of Ca^{2+}	0.4
EuL^4	0.8[a]	EuL^4 + 3 equiv of Ca^{2+}	0.4[a]

[a] ref. [18]

intramolecular rather than an intermolecular process. In this case only one of the phosphonates is available to interact with Ca^{2+} which might explain the smaller and less stable aggregates. None of the luminescence emission spectra of EuL^2−EuL^4 exhibit such a pattern, neither in the absence nor in the presence of Ca^{2+} indicating that the phosphonate groups of these complexes are not coordinated to the lanthanide (Figure 5b).

The hydration number q of EuL^1−EuL^3 was calculated from the luminescence lifetimes in H_2O and D_2O solutions using the equation reported (Table 3),[47] and the resulting values were compared to those previously obtained for EuL^4.[18] For EuL^1, the only complex with a coordinated phosphonate group, a q value of 1.7 is obtained at 5 mM complex concentration in the absence of Ca^{2+}, suggesting the presence of dihydrated species. Since a coordination number of 10 is unlikely for a Eu^{3+} complex, it is indeed possible that a certain amount of species with two noncoordinated phosphonates exists in solution. However, the applied equation is empirical, working already for systems with no second sphere only with an error of ±0.5. Furthermore, the obtained q value might be increased by the influence of additional oscillator(s) brought into the proximity to Eu^{3+} by the coordination of the aminobis(methylenephosphonate) group which is not considered in the calculation of q.[48] Unfortunately it is difficult to estimate the amount of the different influences in this system. By contrast, for EuL^2−EuL^4, the q values are 1 rather than 2 in the absence of Ca^{2+} ions. This does not disagree with the fact that no experimental evidence of a coordination of phosphonates to the paramagnetic center is found, since it is known that nonpolar moieties attached to the fourth cyclen nitrogen can reduce the overall coordination number in water.[49]

The addition of 3 equiv of Ca^{2+} to solutions of EuL^1−EuL^4 reduce q for all four complexes (Table 3). Since the amino nitrogen of the aminobis(methylenephosphonate) groups is protonated at the given conditions, this N−H or N−D moiety is one of these additional oscillators which can influence the luminescene lifetimes and the derived q values. However, it has been shown by pK_a measurements for several aminobis(methylenephosphonates) that the amino nitrogen is not involved in the coordination of Ca^{2+} ions (deprotonation of N−H in the calcium complex occurs only at pH above 10).[26] It is therefore very unlikely that the observed change in q is due to a change in the N−H oscillator. On the other hand, this means that even though the apparent q value might not in all cases represent the exact number of coordinated water molecules in the inner-sphere of these systems, the reduction of the apparent q values must be related to a decreasing number of O−H and O−D oscillators, respectively. This can arise from a lower number of inner-sphere water molecules, as well as from a reduction of second sphere water on the aminobis(methylenephosphonate) groups or a deprotonation of partly protonated phosphonate groups. In all cases the reduction in the obtained q values explains the observed decrease in r_1 for GdL^2− GdL^4, although the relation between q and r_1 is not linear. This is most obvious in the case of LnL^1 were a decrease of 0.5 in q results in hardly any r_1 change at a complex concentration of 5 mM. In contrast to this, for EuL^4 q decreases by only 0.4 whereas the r_1 of GdL^4 for the same concentration decreases from 5.54 mM^{-1} s^{-1} to 3.86 mM^{-1} s^{-1} (−30%).

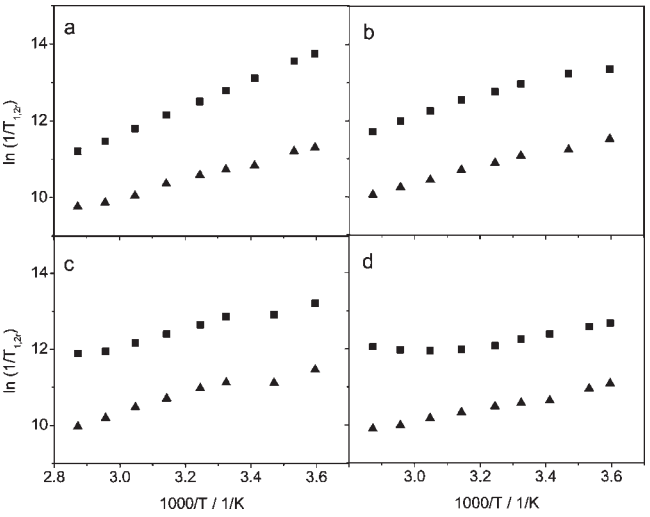

Figure 6. Variable temperature reduced ^{17}O transverse (■) and longitudinal (▲) relaxation rates for (a) GdL^1, (b) GdL^2, (c) GdL^3, (d) GdL^4. B = 11.75 T. q = 1 in all cases.

The hydration number was also determined as a function of the complex concentration (see Supporting Information), and similar trends were observed as for the concentration-dependence of the relaxivities (Figure 3). In the systems where r_1 was independent of the Gd^{3+} complex concentration, q also remained unchanged. However, in all cases were r_1 decreased with increasing complex concentration, the hydration number also dropped for the respective Eu^{3+} complexes. Since the decrease in relaxivity is accompanied with the formation of aggregates, it is assumed that in the so formed structures the water access to the inner and/or second sphere of the lanthanide ion is significantly hindered. The lower number of water molecules being able to interact with the paramagnetic center, is then reflected in the reduced relaxivity. Similarly, Rojas-Quijano et al. reported a decrease of q with increasing complex concentration for the phosphonate containing LnPCTA-$(ampOBu)_3$ which was related to oligomer formation.[50]

^{17}O NMR Spectroscopy. It is a common approach to assess parameters characterizing the water exchange and rotational dynamics on Gd^{3+} complexes by determining their transverse and longitudinal ^{17}O NMR relaxation rates as well as chemical shifts at variable temperatures. We performed the measurements at 11.7 T on the aqueous solutions of GdL^{1-4} at concentrations of about 50 mM. However, the formation of aggregates is likely temperature dependent, thereby possibly altering the investigated system during the measurements at different temperatures. This is obvious in the case of GdL^4 where the $1/T_{2r}$ values at high temperature start to increase (see Figure 6d). Since here the temperature influence on the aggregation state is already reflected in this unusual behavior, we did not perform any further analysis of the ^{17}O NMR data on GdL^4. For complexes GdL^1, GdL^2, and GdL^3 (Figure 6a, 6b, 6c, respectively) no unusual behavior was observed. In all three cases the reduced ^{17}O

dx.doi.org/10.1021/ic1024235 |Inorg. Chem. 2011, 50, 6472–6481

transverse relaxation rates ($1/T_{2r}$) decrease with increasing temperature in the whole temperature range investigated, indicating that they are in the fast exchange region. The experimental data have been fitted to the Solomon−Bloembergen−Morgan theory of paramagnetic relaxation using the equations presented in the Supporting Information. However, since the temperature influence on the aggregation state remains unclear and also the calculation of the exact hydration number is difficult in these systems, the reliability of the calculated parameters has to be challenged. Therefore, the parameters obtained from these measurements are not discussed here in detail, but are given in the Supporting Information.

Independent from the assumed q value (i.e., $q = 1$ or $q = 2$ for **GdL^1** and $q = 1$ or $q = 0.7$ for **GdL^2** and **GdL^3**) the calculated water exchange rates obtained from the fittings are very high. They are in the same order of magnitude as for the $[Gd(H_2O)_8]^{3+}$ aqua ion ($k_{ex}^{298} = 8 \times 10^8\ s^{-1}$). In general, DOTA- or DO3A-type complexes have much slower water exchange rates, though one example of a very fast water exchange has been reported on the Gd^{3+} complex of a DO3A ligand bearing an N-linked CH_2CH_2NHCO-pyridyl moiety ($k_{ex}^{298} = 1.1 \times 10^8\ s^{-1}$).[49] For **LnL^1** the phosphorus NMR data points to a main fraction of molecules with a coordination of one phosphonate group to the lanthanide, which implies an overall coordination number of nine. For that nine-coordinate species, the fast exchange can be related to the presence of the coordinated phosphonate group. Indeed, a coordinated phosphonate group has been often recognized to induce fast water exchange on Gd^{3+} complexes.[21] Here, the water exchange might be further accelerated by the equilibrium between species with a coordinated and species with a noncoordinated phosphonate group. If more than one species is present, the water exchange rate determined from the ^{17}O T_2 data is an averaged value from the two species. In **GdL^2** and **GdL^3**, we assume an overall coordination number of eight with the participation of seven donor groups of the ligand and one inner sphere water molecule for $q = 1$ or even partly 7-fold coordination in the case of $q = 0.7$ (as obtained for higher complex concentrations). Since the common coordination numbers for Gd^{3+} are eight or nine, this would allow for a strongly associative water exchange.

The rotational correlation time τ_{RO}^{298}, as obtained from the analysis of the longitudinal ^{17}O relaxation rates for **GdL^1**, is similar to that calculated from the NMR diffusion experiments for the Y^{3+} analogue. It is longer than τ_{RO}^{298} of GdDOTA which can be explained in terms of a less compact structure brought by the side-chain, a high number of water molecules hydrogen-bound to the bisphosphonate group and a certain amount of aggregated species at this complex concentration. The rotational correlation times of **GdL^2** and **GdL^3** depend on the q assumed, but in any case, they are longer than that for **GdL^1**, which is indicative of stronger aggregation. For **GdL^1**, we have also measured the longitudinal ^{17}O relaxation rates in the presence of 3 equiv of calcium. The $1/T_{1r}$ values were higher than in the absence of Ca^{2+}, in accordance with a longer rotational correlation time affirming the calcium-induced aggregation.

CONCLUSION

We have synthesized a series of novel DO3A-type gadolinium complexes, provided with alkylaminobis(methylene-phosphonate) moieties for interaction with Ca^{2+}. At low complex concentrations (2.5 mM), the longitudinal relaxivity of **GdL^2**−**GdL^4** decreases after addition of Ca^{2+}, whereas **GdL^1** displays no calcium dependence. Concentration-dependent relaxivity and diffusion measurements show that calcium-induced aggregation is responsible for the observed changes in relaxivity.[51] **GdL^1** has a lower tendency to form aggregates in the presence of calcium than **GdL^2**−**GdL^4**, resulting in a calcium dependent relaxivity change only at high complex concentrations. This is attributed to a different coordination behavior of the phosphonate groups in **GdL^1** as compared to **GdL^2**−**GdL^4**: ^{31}P NMR spectroscopy and luminescence measurements on the europium analogues demonstrated a coordination of one phosphonate group to the lanthanide ion for **GdL^1**, but not for **GdL^2**−**GdL^4**. For **GdL^2**−**GdL^4**, this likely allows the involvement of both phosphonate groups in the calcium-induced aggregate formation, resulting in larger and more stable aggregates. The formation of dimers and the metal-induced formation of larger aggregates is a well-described phenomenon for aminobisphosphonates.[26,35] Such aggregation has an impact on the water access to the inner and/or the second sphere of the lanthanide complexes, which is reflected by a reduction in the apparent hydration number q. Structural models have been proposed for these interactions involving intermolecular metal bridges between phosphonate oxygens and amino groups.[26] We should note that the increase of the rotational correlation time upon Ca^{2+} addition is likely not enough to lead to any detectable change in the proton relaxivities at the high magnetic field used in this study.

Despite the uncertainty accompanied with a likely temperature-dependence of the aggregate formation, variable temperature ^{17}O NMR measurements indicate an extremely high water exchange rate k_{ex}^{298} for these complexes, being in the same order of magnitude as that of the $[Gd(H_2O)_8]^{3+}$ aqua ion. Both **GdL^3** and **GdL^4** show a relaxivity increase upon decrease in Ca^{2+} concentration (at low **GdL^n** concentration), which has not been reported so far for a gadolinium-based Ca^{2+} responsive SCA. In terms of potential MRI applications, this behavior would be favorable for tracking the changes in the extracellular Ca^{2+}. Namely, its concentration drops during the neuronal activity,[52] and such changes could be followed by the increase in the relaxivity of **GdL$^{3-4}$** and thus the increase in the resulting MR signal. However, the previous in vivo study on **GdL^4** indicated that this intricate mechanism which is responsible for the relaxivity change is impeded in the living rat brain.[18] The performed studies and their results demonstrate that structurally relatively simple lanthanide complexes might have unexpected and complicated solution chemistry behavior. Nevertheless, the quest for responsive SCAs can be further enriched with such novel approaches and the resulting complexes.

ASSOCIATED CONTENT

Supporting Information. Relaxometric Ca^{2+} titration data of **GdL^1**−**GdL^4**; ^{31}P NMR spectra of **EuL^1** and **EuL^4**; luminescence emission spectra of **EuL^2** and **EuL^3**; concentration dependent emission lifetimes and estimated q values of **EuL^1**−**EuL^4** in the absence and presence of 3 equiv of Ca^{2+}; potentiometric titration curves of **GdL^1**−**GdL^4**; temperature dependent ^1H T_1 relaxation rates of **GdL^4**; temperature dependent ^{17}O T_2 relaxation times of **GdL^4**; equations used in the analysis of the ^{17}O NMR data; parameters obtained from the ^{17}O NMR data of **GdL$^{1-3}$**; variable temperature reduced longitudinal and transverse ^{17}O relaxation rate and chemical shift data of **GdL^1**−**GdL^4**. This material is available free of charge via the Internet at http://pubs.acs.org.

AUTHOR INFORMATION

Corresponding Author

*Phone: +49 7071 601 916 (G.A.), +49 7071 29 76229 (H.A.M.). Fax: +49 7071 29 2436 (H.A.M.). E-mail: goran.angelovski@tuebingen.mpg.de (G.A.), hermann.mayer@uni-tuebingen.de (H.A.M.).

Author Contributions

⊥These authors equally contributed to this work.

ACKNOWLEDGMENT

The authors thank Dr. J. Pfeuffer for helpful discussions. J.H. thanks the Fonds der Chemischen Industrie for a Ph.D. scholarship. This work is funded by the Max-Planck Society, the Hertie Foundation, the Louis-Jeantet Foundation, and the Centre National de la Recherche Scientifique (CNRS, France) and has been performed within the frame of the European COST Action D38 "Metal-Based Systems for Molecular Imaging Applications".

REFERENCES

(1) *The Chemistry of Contrast Agents in Medical Magnetic Resonance Imaging*; Tóth, É., Merbach, A. E., Eds.; Wiley: Chichester, 2001.

(2) Caravan, P.; Ellison, J. J.; McMurry, T. J.; Lauffer, R. B. *Chem. Rev.* **1999**, *99*, 2293–2352.

(3) Jasanoff, A. *Curr. Opin. Neurobiol.* **2007**, *17*, 593–600.

(4) Yoo, B.; Pagel, M. D. *Front. Biosci.* **2008**, *13*, 1733–1752.

(5) Zhang, S. R.; Wu, K. C.; Sherry, A. D. *Angew. Chem., Int. Ed.* **1999**, *38*, 3192–3194.

(6) Woods, M.; Kiefer, G. E.; Bott, S.; Castillo-Muzquiz, A.; Eshelbrenner, C.; Michaudet, L.; McMillan, K.; Mudigunda, S. D. K.; Grin, D.; Tircso, G.; Zhang, S. R.; Zhao, P.; Sherry, A. D. *J. Am. Chem. Soc.* **2004**, *126*, 9248–9256.

(7) Mamedov, I.; Mishra, A.; Angelovski, G.; Mayer, H. A.; Palsson, L. O.; Parker, D.; Logothetis, N. K. *Dalton Trans.* **2007**, 5260–5267.

(8) Garcia-Martin, M. L.; Martinez, G. V.; Raghunand, N.; Sherry, A. D.; Zhang, S.; Gillies, R. J. *Magn. Reson. Med.* **2006**, *55*, 309–315.

(9) Angelovski, G.; Fouskova, P.; Mamedov, I.; Canals, S.; Toth, E.; Logothetis, N. K. *ChemBioChem* **2008**, *9*, 1729–1734.

(10) Dhingra, K.; Maier, M. E.; Beyerlein, M.; Angelovski, G.; Logothetis, N. K. *Chem. Commun.* **2008**, 3444–3446.

(11) Li, W. H.; Fraser, S. E.; Meade, T. J. *J. Am. Chem. Soc.* **1999**, *121*, 1413–1414.

(12) Hanaoka, K.; Kikuchi, K.; Urano, Y.; Narazaki, M.; Yokawa, T.; Sakamoto, S.; Yamaguchi, K.; Nagano, T. *Chem. Biol.* **2002**, *9*, 1027–1032.

(13) Hanaoka, K.; Kikuchi, K.; Urano, Y.; Nagano, T. *J. Chem. Soc., Perkin Trans. 2* **2001**, 1840–1843.

(14) Major, J. L.; Parigi, G.; Luchinat, C.; Meade, T. J. *Proc. Natl. Acad. Sci. U. S. A.* **2007**, *104*, 13881–13886.

(15) Major, J. L.; Boiteau, R. M.; Meade, T. J. *Inorg. Chem.* **2008**, *47*, 10788–10795.

(16) Zhang, X. A.; Lovejoy, K. S.; Jasanoff, A.; Lippard, S. J. *Proc. Natl. Acad. Sci. U. S. A.* **2007**, *104*, 10780–10785.

(17) Dhingra, K.; Fouskova, P.; Angelovski, G.; Maier, M. E.; Logothetis, N. K.; Tóth, É. *JBIC* **2008**, *13*, 35–46.

(18) Mamedov, I.; Canals, S.; Henig, J.; Beyerlein, M.; Murayama, Y.; Mayer, H. A.; Logothetis, N. K.; Angelovski, G. *ACS Chem. Neurosci.* **2010**, *1*, 819–828.

(19) Kotková, Z.; Pereira, G. A.; Djanashvili, K.; Kotek, J.; Rudovský, J.; Hermann, P.; Elst, L. V.; Muller, R. N.; Geraldes, C. F. G. C.; Lukes, I.; Peters, J. A. *Eur. J. Inorg. Chem.* **2009**, 119–136.

(20) Helm, L. *Prog. Nucl. Magn. Reson. Spectrosc.* **2006**, *49*, 45–64.

(21) Hermann, P.; Kotek, J.; Kubicek, V.; Lukes, I. *Dalton Trans.* **2008**, 3027–3047.

(22) Kubicek, V.; Rudovsky, J.; Kotek, J.; Hermann, P.; Elst, L. V.; Muller, R. N.; Kolar, Z. I.; Wolterbeek, H. T.; Peters, J. A.; Lukes, I. *J. Am. Chem. Soc.* **2005**, *127*, 16477–16485.

(23) Adzamli, I. K.; Blau, M.; Pfeffer, M. A.; Davis, M. A. *Magn. Res. Med.* **1993**, *29*, 505–511.

(24) Westerback, S. J.; Martell, A. E. *Nature* **1956**, *178*, 321–322.

(25) Bugłyo, P.; Kiss, T.; Dyba, M.; Jezowska-Bojczuk, M.; Kozlowski, H.; Bouhsina, S. *Polyhedron* **1997**, *16*, 3447–3454.

(26) Matczak-Jon, E.; Kurzak, B.; Kamecka, A.; Sawka-Dobrowolska, W.; Kafarski, P. *J. Chem. Soc., Dalton Trans.* **1999**, 3627–3637.

(27) Corsi, D. M.; Platas-Iglesias, C.; van Bekkum, H.; Peters, J. A. *Magn. Reson. Chem.* **2001**, *39*, 723–726.

(28) Irving, H. M.; Miles, M. G.; Pettit, L. D. *Anal. Chim. Acta* **1967**, *38*, 475–488.

(29) Zekany, L., Nagypal, I. *Computational methods for the determination of formation constants*; Plenum Press: New York, 1985.

(30) Zitha-Bovens, E.; Vander Elst, L.; Muller, R. N.; van Bekkum, H.; Peters, J. A. *Eur. J. Inorg. Chem.* **2001**, 3101–3105.

(31) Peters, J. A.; Huskens, J.; Raber, D. J. *Prog. Nucl. Magn. Reson. Spectrosc.* **1996**, *28*, 283–350.

(32) Raiford, D. S.; Fisk, C. L.; Becker, E. D. *Anal. Chem.* **1979**, *51*, 2050–2051.

(33) Hedrera, M. E.; Perillo, I. A. *J. Heterocycl. Chem.* **2000**, *37*, 1431–1438.

(34) Moedritz., K.; Irani, R. R. *J. Org. Chem.* **1966**, *31*, 1603–1607.

(35) Matczak-Jon, E.; Kurzak, B.; Kafarski, P.; Wozna, A. *J. Inorg. Biochem.* **2006**, *100*, 1155–1166.

(36) Alajarín, M.; Pastor, A.; Orenes, R.-A.; Martínez-Viviente, E.; Pregosin, P. S. *Chem.—Eur. J.* **2006**, *12*, 877–886.

(37) Cohen, Y.; Avram, L.; Frish, L. *Angew. Chem., Int. Ed.* **2005**, *44*, 520–554.

(38) Macchioni, A.; Ciancaleoni, G.; Zuccaccia, C.; Zuccaccia, D. *Chem. Soc. Rev.* **2008**, *37*, 479–489.

(39) Mamedov, I.; Parac-Vogt, T. N.; Logothetis, N. K.; Angelovski, G. *Dalton Trans.* **2010**, *39*, 5721–5727.

(40) Valentini, M.; Rüegger, H.; Pregosin, P. S. *Helv. Chim. Acta* **2001**, *84*, 2833–2853.

(41) Henig, J.; Tóth, É.; Engelmann, J.; Gottschalk, S.; Mayer, H. A. *Inorg. Chem.* **2010**, *49*, 6124–6138.

(42) Yao, S.; Babon, J. J.; Norton, R. S. *Biophys. Chem.* **2008**, *136*, 145–151.

(43) Livramento, J. B.; Weidensteiner, C.; Prata, M. I. M.; Allegrini, P. R.; Geraldes, C. F. G. C.; Helm, L.; Kneuer, R.; Merbach, A. E.; Santos, A. C.; Schmidt, P.; Tóth, É. *Contrast Med. Mol. Imaging* **2006**, *1*, 30–39.

(44) Aime, S.; Botta, M.; Garino, E.; Crich, S. G.; Giovenzana, G.; Pagliarin, R.; Palmisano, G.; Sisti, M. *Chem.—Eur. J.* **2000**, *6*, 2609–2617.

(45) Atkinson, P.; Bretonniere, Y.; Parker, D. *Chem. Commun.* **2004**, 438–439.

(46) Atkinson, P.; Murray, B. S.; Parker, D. *Org. Biomol. Chem.* **2006**, *4*, 3166–3171.

(47) Beeby, A.; Clarkson, I. M.; Dickins, R. S.; Faulkner, S.; Parker, D.; Royle, L.; de Sousa, A. S.; Williams, J. A. G.; Woods, M. *J. Chem. Soc., Perkin Trans. 2* **1999**, 493–503.

(48) Supkowski, R. M.; Horrocks, W. D. *Inorg. Chim. Acta* **2002**, *340*, 44–48.

(49) Congreve, A.; Parker, D.; Gianolio, E.; Botta, M. *Dalton Trans.* **2004**, 1441–1445.

(50) Rojas-Quijano, F. A.; Benyo, E. T.; Tircso, G.; Kalman, F. K.; Baranyai, Z.; Aime, S.; Sherry, A. D.; Kovacs, Z. *Chem.—Eur. J.* **2009**, *15*, 13188–13200.

(51) Kubicek, V.; Vitha, T.; Kotek, J.; Hermann, P.; Vander Elst, L.; Muller, R. N.; Lukes, I.; Peters, J. A. *Contrast Med. Mol. Imaging* **2010**, *5*, 294–296.

(52) Nicholson, C.; ten Bruggencate, G.; Stockle, H.; Steinberg, R. *J. Neurophysiol.* **1978**, *41*, 1026–1039.